**Showcasing research from Dr. André Schäfer's laboratory, Department of Chemistry, Saarland University, Germany.**

Bis(di-*tert*-butylindenyl)tetrelocenes

While indenyl is an important ligand in transition metal chemistry and many transition metal bis(indenyl) metallocenes have been reported, bis(indenyl)tetrelocenes are almost unexplored. In this contribution, a series of bis(di-*tert*-butylindenyl) germanium(II), tin(II) and lead(II) complexes is reported, which includes the first structurally authenticated example of a bis(indenyl)germanocene.

Check for updates
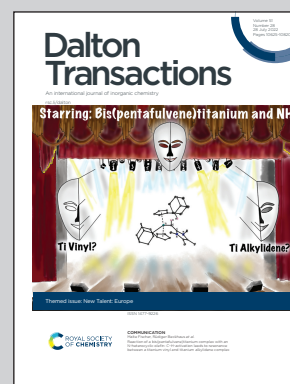
Bis(di-*tert*-butylindenyl)tetrelocenes†

Liane Hildegard Staub,‡[a] Jessica Lambert,‡[a] Carsten Müller,[a] Bernd Morgenstern,[a] Michael Zimmer,[a] Joshua Warken,[a] Aylin Koldemir,[b] Theresa Block,[b] Rainer Pöttgen [ID][b] and André Schäfer [ID] *[a]

The synthesis and characterization of bis(di-*tert*-butylindenyl) germanium(II), tin(II) and lead(II) complexes are reported, which includes the first structurally authenticated example of a bis(indenyl)germanocene. The species were studied in detail in solution and in the solid, which includes single crystal X-ray diffraction and NMR spectroscopy, as well as Mössbauer spectroscopy of the tin compound.
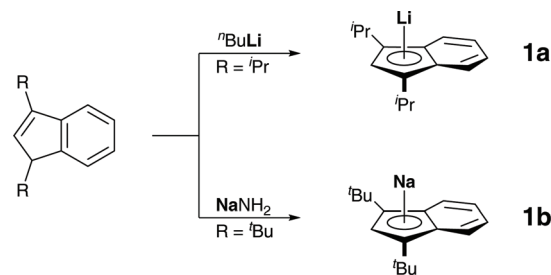
Introduction

Since the report of bis(indenyl)ferrocene, Ind_2Fe, and bis(indenyl)cobaltocene, Ind_2Co, in 1954,[1] just a few years after the discovery of its parent compound, Cp_2Fe,[2] indenyl has developed into an important ligand in transition metal chemistry and many indenyl-based metallocenes have been reported, ever since.[3] On the other hand, although group 14 metallocenes (tetrelocenes) have been known for many decades, it is rather surprising that bis(indenyl)tetrelocenes are almost unexplored.[4] This might be related to the tendency of the indenyl ligand to adopt an η^3 rather than an η^5 coordination mode in some cases – often referred to as the indenyl effect[5] – presumably making these compounds less stable than their cyclopentadienyl counterparts. To date, only a handful of bis(indenyl)tetrelocenes have been reported and only two of them have been structurally authenticated, namely a bis(bis(trimethylsilyl)indenyl)stannocene and a bis(bis(trimethylsilyl)indenyl)plumbocene. In addition, bis(bis(trimethylsilyl)indenyl)germanocene and bis(diisopropylindenyl) plumbocene have been characterized by NMR spectroscopy in solution, even though the latter was described to be unstable at ambient conditions, decomposing under the formation of elemental lead after just a few minutes. Furthermore, some related mixed heteroleptic indenyl cyclopentadienyl derivatives have also been described.[6]

Following our group's continued interest in main group metallocene chemistry, we investigate the applicability of diisopropylindenyl and di-*tert*-butylindenyl as ligands for heavier group 14 elements and herein report the synthesis and structural characterization of a series of bis(di-*tert*-butylindenyl) tetrelocenes of germanium, tin and lead.

Results and discussion

We started our investigation by preparing diisopropylindene and di-*tert*-butylindene, followed by metalations with *n*-butyllithium and sodium amide, as described in the literature (Scheme 1).[7]

Crystals of these alkaline metal indenyl complexes, **1a,b**, suitable for X-ray diffraction, could be obtained from dimethoxyethane solutions at 273 K and allowed for structural characterizations (Fig. 1). **1a·**(dme) crystallized in the triclinic space group $P\bar{1}$, while **1b·**(dme)$_3$ crystallized in the monoclinic space group $P2_1/c$, both with one formular unit per asymmetric unit ($Z = 1$). Interestingly, while both compounds crystallize as dimethoxyethane complexes, lithium diisopropylindenide **1a** forms a mono(dimethoxyethane) contact ion pair complex, while sodium di-*tert*-butylindenide **1b** forms solvent separated

*[a]Department of Chemistry, Faculty of Natural Sciences and Technology, Saarland University, Campus Saarbrücken, 66123 Saarbrücken, Germany.
E-mail: andre.schaefer@uni-saarland.de*
[b]Institute of Inorganic and Analytical Chemistry, Westfälische Wilhelms-Universität Münster, Corrensstrasse 30, 48149 Münster, Germany

‡These authors contributed equally.

Scheme 1 Synthesis of lithium diisopropyl indenide, **1a**, and sodium di-*tert*-butyl indenide, **1b**.
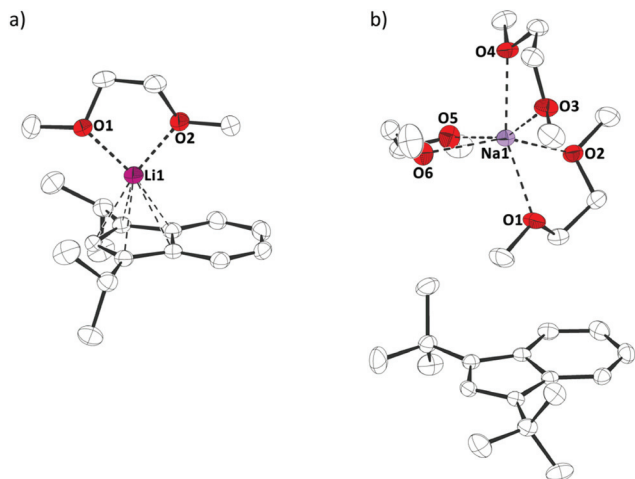
Fig. 1 Molecular structure of (a) **1a**·(dme) and (b) **1b**·(dme)$_3$ in the crystal (displacement ellipsoids at 50% probability level, H-atoms omitted for clarity).

ion pairs with three dimethoxyethane molecules coordinated to the sodium ion. This might be related to the increased steric demand of the di-*tert*-butylindenyl ligand compared to diisopropylindenyl and to a more ionic sodium indenyl bonding interaction compared to the lithium indenyl bonding.

The Li–Ind^{centroid} bonding distance in **1a**·(dme) is 194.35(43) pm, which is slightly shorter than in lithium bis(tetrahydrofuran) bis(trimethylsilyl)indenide[6c] (199.79(62) pm), but longer than in lithium dimethoxyethane cyclopentadienide[8] (190.98(29) pm). Characterization of lithium dimethoxyethane diisopropyl-indenide, **1a**·(dme), by ^{7}Li NMR spectroscopy in solution (C$_6$D$_6$) and in the solid state revealed quasi-identical ^{7}Li NMR chemical shifts (δ^7Li(C$_6$D$_6$) = −8.8; (δ^7Li(CP-MAS) = −8.2), indicating that the complex is stable in benzene solutions (Fig. 2).

Following the successful synthesis of lithium diisopropyl-indenide **1a** and sodium di-*tert*-butylindenide **1b**, we investigated the reactivity of these compounds toward group 14 diha-
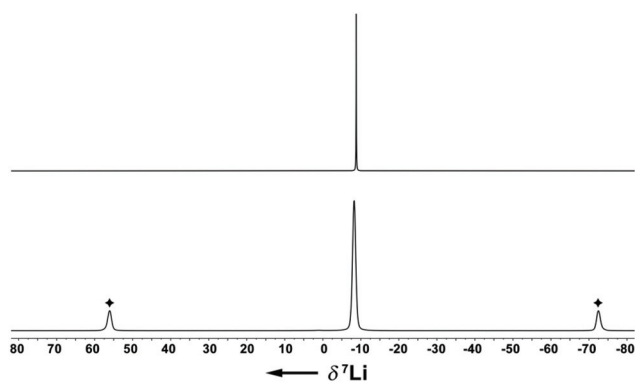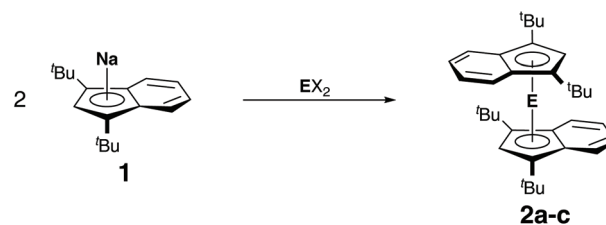
lides. Hanusa *et al.* had already reported that the reaction of potassium indenide or potassium diisopropylindenide with lead(II) iodide did not yield stable complexes, but resulted in the formation of lead metal.[6b] Likewise, an attempt by us to react bis(indenyl)magnesocene[9] with germanium(II) chloride dioxane only yielded a complex mixture of unidentifiable products, indicating that the unsubstituted bis(indenyl)tetrelocenes are not stable. As stated before, this might be related to the indenyl effect,[5] as the associated tendency of η^5 to η^3 ring-slippage may result in weaker E–Ind bonds compared to E–Cp bonds. However, it must also be taken into consideration that electronic effect can play a role here, as 1,3-di-*tert*-butylindenide is more electron rich than unsubstituted indenide, which promotes stronger bonding. Nevertheless, we attempted the synthesis of the bis(diisopropylindenyl)tetrelocenes, starting from **1a** and germanium(II) chloride, tin(II) chloride and lead(II) chloride, but in all cases only obtained complex mixtures of products, in case of tin and lead containing large amounts of diisopropylindene along with metallic tin and lead. Thus, we turned to the sterically more demanding di-*tert*-butylindenyl ligand. Indeed, the reactions of sodium di-*tert*-butylindenide, **1b**, with germanium(II) chloride, tin(II) chloride and lead(II) bromide yielded the corresponding tetrelocenes as air and moisture sensitive, but somewhat stable and isolatable solids (Scheme 2). Noteworthy, we found that shorter reaction times in case of the synthesis of plumbocene **2c** were extremely beneficial. Stirring the reaction mixture over night yielded almost no product and large amount of lead metal, while rapid workup after just 15 minutes gave plumbocene **2c** in good yields, indicating that **2c** exhibits only limited stability in solution.

Crystals of tetrelocenes **2a–c**, suitable for X-ray diffraction, were obtained at low temperatures and allowed for structural characterization of these species (Fig. 3). **2a–c** all crystallized in the same monoclinic space group $P2_1/n$, each with one molecule per asymmetric unit ($Z = 1$). Interestingly, the previously reported solid state structures of bis(bis(trimethylsilyl)indenyl)stannocene[6c] and bis(bis(trimethylsilyl)indenyl)plumbocene[6b] showed tilted geometries in the solid state ($\alpha = 17.1°$ to 20.9°), analogous to many other tetrelocenes, while almost parallel arrangements are observed in **2a–c** ($\alpha = 3.1°$ to 4.4°). The tetrel indenyl–centroid bonding distances are similar between **2b,c** and their trimethylsilyl derivatives, only marginally elongated compared to their unsubstituted Cp$_2$E-type

Fig. 2 ^{7}Li{^{1}H} NMR spectra of **1a**·(dme) (upper trace: C$_6$D$_6$ solution, 156 MHz, 295 K; lower trace: CP-MAS(10 kHz), 156 MHz, 297 K; ✦ spinning sidebands).

Scheme 2 Synthesis of indenyl tetrelocenes **2a–c** (**a**: EX$_2$ = GeCl$_2$; **b**: EX$_2$ = SnCl$_2$; **c**: EX$_2$ = PbBr$_2$).
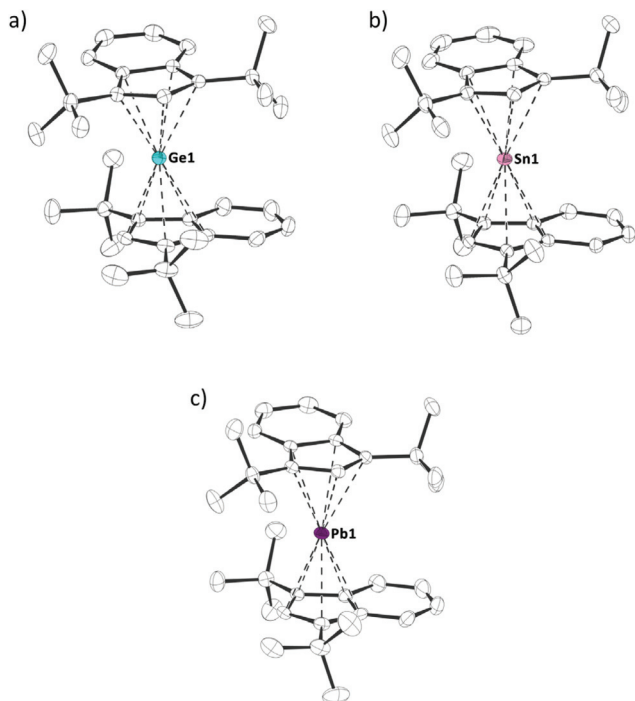
Fig. 3 Molecular structure of indenyl tetrelocenes (a) **2a**, (b) **2b** and (c) **2c** in the crystal (displacement ellipsoids at 50% probability level, H-atoms omitted for clarity, only one of two rotamers shown).

parent compounds, and – as to be expected – increase going from germanium to lead. Furthermore, the two indenyl ligands are twisted against each other, with torsions angles of 83.2° to 92.2° (Table 1 and Fig. 3). Due to this twisting, two

different rotamers exist and **2a–c** are formally axial chiral in the solid state and crystallize as racemates, thus both rotamers/enantiomers are observed in the crystals.[10]

In addition to a NMR characterization of **2a–c** in solution, we also studied stannocene **2b** and plumbocene **2c** by CP/MAS NMR spectroscopy in the solid state (Fig. 5). The ^{119}Sn NMR chemical shift of **2b** is only slightly shifted between solution and solid state, with $\Delta\delta^{119}$Sn = 63, but both resonances (δ^{119}Sn (C$_6$D$_6$) = −2272; δ^{119}Sn(CP/MAS) = −2335) are within the typical range of stannocene-type compounds[13] and are similar to the ^{119}Sn NMR chemical shift of bis(bis(trimethylsilyl) indenyl)stannocene, reported by Jones and Cowley (δ^{119}Sn (C$_6$D$_6$) = −2168.[6c] Furthermore, chemical shift tensors of δ_{11} =
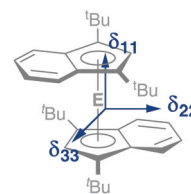

Fig. 4 Schematic depiction of the principal axes of the chemical shift tensors δ_{11}, δ_{22} and δ_{33} in **2a–c**.

Table 1 Selected structural parameters and NMR chemical shifts of indenyl tetrelocenes **2a–c** and related compounds

Compound	E–Ind/Cp[a] [pm]	α^b [°]	θ^c [°]	δ^{119}Sn/δ^{207}Pb
2a	225.21(5)	4.4	83.2	—
	225.41(5)			
2b	241.08(3)	3.8	91.8	−2272[d]
	242.13(3)			−2335[e]
2c	247.72(3)	3.1	92.2	−4503[f]
	248.55(3)			−4734[g]
(^{2Si}Ind)$_2$Sn[6c]	241.24(7)	20.3	79.2	−2121[6c]
	241.94(7)	20.9	83.4	
	242.84(7)			
	242.95(7)			
(^{2Si}Ind)$_2$Pb[6b]	248.34(7)	17.1	79.4	—
	248.50(7)	18.1	83.1	
	248.51(7)			
	248.86(7)			
Cp$_2$Ge[11]	223.37(43)	50.2	—	—
Cp$_2$Sn[12]	237.02(8)	45.9		−2199[13]
	241.04(9)	46.7		
	243.69(8)			
Cp$_2$Pb[14]	246.55(5)	57.5		−5030[15]

[a] Relative to centroid of C$_5$ moiety. [b] Dihedral angle between cyclopentadienide or indenide planes. [c] C^{Ind}–centroid^{Ind}–centroid^{Ind}–C^{Ind} torsion angle. [d] 149 MHz, C$_6$D$_6$, 295 K. [e] 149 MHz, CP-MAS (13 kHz). [f] 83 MHz, C$_6$D$_6$, 294 K. [g] 83 MHz, CP-MAS (13 kHz).
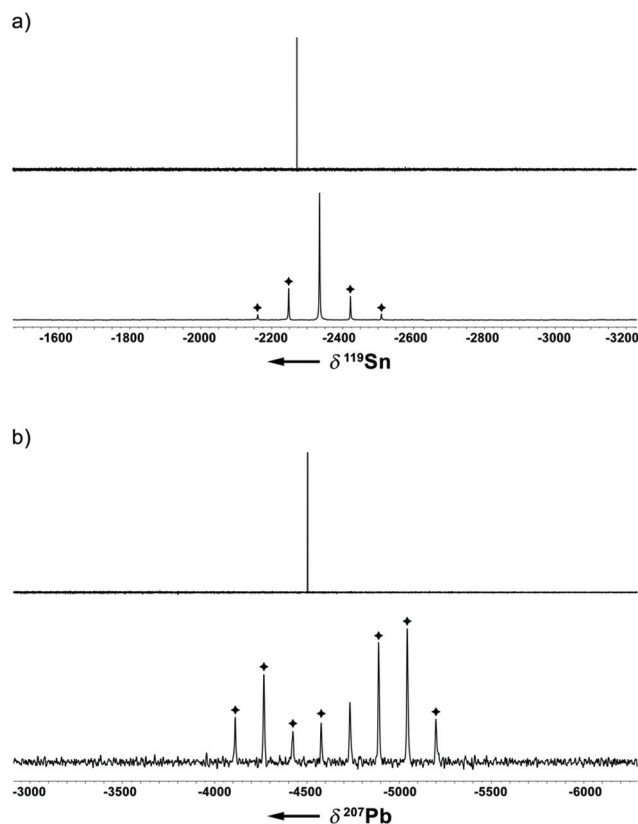

Fig. 5 (a) ^{119}Sn{^{1}H} NMR spectra of **2b** (upper trace: C$_6$D$_6$ solution, 149 MHz; lower trace: CP-MAS (13 kHz), 149 MHz; ✦ spinning sidebands) and (b) [207]Pb{^{1}H} NMR spectra of **2c** (upper trace: C$_6$D$_6$ solution, 83 MHz, 294 K; lower trace: CP-MAS (13 kHz), 83 MHz; ✦ spinning sidebands).

-2216, $\delta_{22} = -2318$ and $\delta_{33} = -2470$ are found, whereby the more deshielded component δ_{11} corresponds to the tensor along the Ind–Sn–Ind axis (Fig. 4). Hence, a chemical shift span of $\Omega = \delta_{11} - \delta_{33} = 102$, which implies a smaller chemical shift anisotropy than in many stannylene-type compounds, is observed.[16]

Noteworthy, no [207]Pb NMR chemical shift of a bis(indenyl) plumbocene has been reported yet, as Hanusa *et al.* did not describe [207]Pb NMR chemical shifts for bis(diisopropylindenyl)plumbocene or bis(bis(trimethylsilyl)indenyl)plumbocene.[6b] Within this work, we can confirm that the [207]Pb NMR chemical shifts for 2c in solution and in the solid state (δ^{207}Pb (C_6D_6) = -4503; δ^{207}Pb(CP/MAS) = -4734) are within the typical range of Cp-based plumbocenes (*e.g.*: δ^{207}Pb(Cp$_2$Pb) = -5030; δ^{207}Pb(Cp$^*_2$Pb) = -4384.[15,17] Furthermore, the resonance of 2c is shifted by $\Delta\delta^{207}$Pb = 231, compared to the resonance observed in solution, with chemical shift tensors of δ_{11} = -3891 and $\delta_{22} = \delta_{33} = -5169$, resulting in a chemical shift span of $\Omega = \delta_{11} - \delta_{33} = 1278$, which is a similar pattern to what was observed for stannocene 2b.

In addition to characterization by NMR spectroscopy, we also performed [119]Sn Mössbauer spectroscopy on stannocene 2b at 78 K (Fig. 6). The corresponding fitting parameters are summarized in Table 2. Noteworthy, to the best of our knowledge, this is the first characterization of an indenyl tin(II) complex by Mössbauer spectroscopy, even though Mössbauer spectroscopy of Cp$_2$Sn-type stannocenes has been reported.[18]

The experimental Mössbauer spectrum is well reproduced with three subsignals. Signal A with the highest signal intensity can be assigned to stannocene 2b, while signal B and C

can be attributed to decomposition products of this compound. Because of the identical chemical environment for all tin(II) atoms in stannocene 2b, a single signal (A) is expected. The isomer shift of $\delta = 3.80(1)$ mm s^{-1} is close to isomer shifts of Cp-based stannocenes (δ(Cp$_2$Sn) = 3.73(6) mm s^{-1}; δ(Me$_4$Si$_2$[2]Cp$_2$Sn) = 3.734(6) mm s^{-1}.[18a,c] Thus, there is no strong effect of the indenyl ligand on the isomer shift compared to cyclopentadienyl. This means that s electron density of tin(II) is predominantly affected by the C_5 moiety of the di-*tert*-butylindenyl ligand. The coplanar (linear with regards to the centroids) coordination of tin(II) in 2b causes the small electric quadrupole splitting of $\Delta E_Q = 0.70(1)$ mm s^{-1}, which is also close to the reported one for Cp$_2$Sn ($\Delta E_Q = 0.65(6)$ mm s^{-1} (ref. 18a)). Signal B with an isomer shift of $\delta = 0.14(2)$ mm s^{-1} and a quadrupole splitting of $\Delta E_Q = 0.63(3)$ mm s^{-1} is within the typical range of Sn(IV) compounds. Therefore, we assume that signal B can be assigned to SnO$_2$, or, respectively, organotin oxygen derivates resulting from hydrolysis and/or oxidation of 2b.[19–21] Signal C shows an isomer shift of $\delta = 2.80(1)$ mm s^{-1} and a quadrupole splitting of $\Delta E_Q = 2.03(3)$ mm s^{-1} which is comparable to the Mössbauer spectroscopic data of Sn(OH)$_2$ ($\delta = 2.83(6)$ mm s^{-1}; $\Delta E_Q = 2.20(6)$ mm s^{-1} or other organotin hydroxide byproducts,[20–22] which may also result from hydrolysis of 2b. All observed line widths are in the usual range for [119]Sn Mössbauer spectroscopic investigations.[19,20]

Following our experimental investigation, we also conducted DFT calculations at the PBE0-D3/def2-TZVP level of theory,[23] choosing germanocene 2a as a model compound, since little was known about the frontier orbitals of bis(indenyl)-tetrelocenes. The calculated structure is in good agreement with the experimentally determined solid-state structure, with the Ge–Ind^{centroid} bonds being marginally shorter by *ca.* 2 pm in the solid-state structure. Inspection of the frontier orbitals of germanocene 2a reveals a picture typical for tetrelocenes (Fig. 7).

The LUMO has a large coefficient at the central atom in the shape of a p orbital and is antibonding in nature with regards to the Ge–Ind bonds. As to be expected from the quasi-coplanar geometry of the indenyl ligands, the formal lone pair at the central atom possesses a spherical shape due to its high s character and is also anti-bonding with regards to the germa-
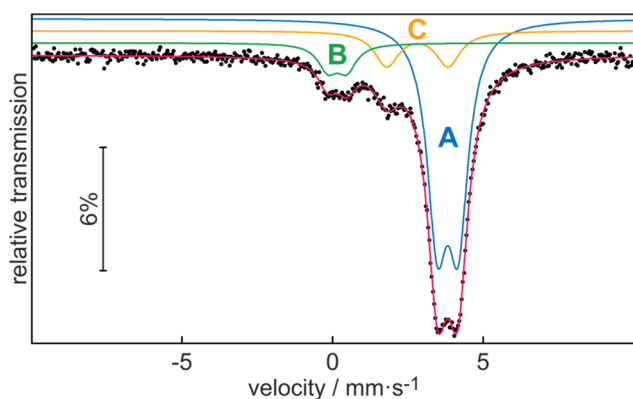

Fig. 6 Experimental and simulated [119]Sn Mössbauer spectrum of 2b.

Table 2 Fitting parameters of the [119]Sn Mössbauer spectroscopic measurement for 2b at 78 K. δ = isomer shift, ΔE_Q = electric quadrupole splitting, Γ = experimental line width

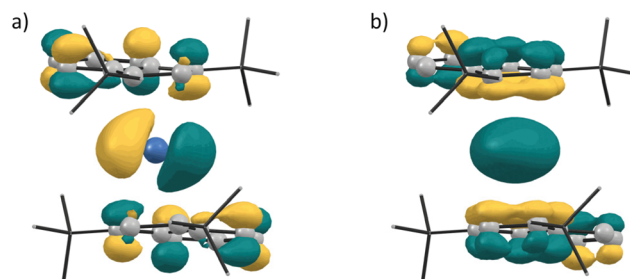| Signal	δ [mm s^{-1}]	ΔE_Q [mm s^{-1}]	Γ [mm s^{-1}]	Area [%]
A	3.80(1)	0.70(1)	0.81(1)	75(1)
B	0.14(2)	0.63(3)	0.78(6)	9(1)
C	2.80(1)	2.03(3)	0.98(6)	16(1)

Fig. 7 Kohn–Sham molecular orbital contours of (a) LUMO and (b) HOMO−4 of 2a (calculated at PBE0-D3/def2-TZVP; isodensity = 0.045 a.u.).

nium indenyl bonds and relatively low in energy, being the HOMO−4.

Conclusions

In this work we studied the underexplored class of bis(indenyl) complexes of group 14 elements in oxidation state +II and found that these bis(indenyl)tetrelocenenes are only stable with a sterically demanding 1,3-substitution pattern. Utilizing the 1,3-di-*tert*-butylindenyl ligand in the form of its sodium complex, **1b**, we were able to prepare the corresponding series of germanocene, **2a**, stannocene, **2b**, and plumbocene, **2c**. The compounds were characterized by multinuclear NMR spectroscopy and single crystal X-ray diffraction, as well as ^{119}Sn Mössbauer spectroscopy in case of **2b**. They exhibit ^{119}Sn and ^{207}Pb NMR and ^{119}Sn Mössbauer parameters, which are similar to Cp-based stannocenes and plumbocenes, respectively. Noteworthy, germanocene **2a** represents the first X-ray diffraction structurally authenticated example of a bis(indenyl) germanocene.

Experimental

All manipulations were carried out under an argon inert gas atmosphere (argon 5.0), using Schlenk techniques and a glovebox. Diisopropyl indene and di-*tert*-butyl indene were prepared following literature procedures.[8]

NMR spectra were recorded on Bruker Avance III 300 (solution), Bruker Avance III 400 (solution) and Bruker Ascend 400WB (solid state) spectrometers. ^{1}H and ^{13}C NMR spectra were referenced using the solvent signals,[24] ^{7}Li, ^{119}Sn and ^{207}Pb NMR spectra were referenced using external standards (δ^{7}Li(LiCl in D$_2$0) = 0; δ^{119}Sn(Me$_4$Sn) = 0; δ^{207}Pb(Me$_4$Pb) = 0).

Single crystal X-ray diffraction analysis were carried out on a Bruker D8 Venture diffractometer with a microfocus sealed tube and a Photon II detector and using monochromated MoK$_\alpha$ radiation (λ = 0.71073 Å). Corrected for absorption effects was performed with the multi-scan method. The structure was solved by direct methods using SHELXT and was refined by full matrix least squares calculations on F^2 (SHELXL 2018) in the graphical user interface ShelXle.[25−28] Crystal structure data has been deposited in the Cambridge Structural Database at CCDC 2154213–2154217.† ^{119}Sn Mössbauer spectroscopy was performed with a Ca^{119m}SnO$_3$ source in normal transmission geometry for three days, whereby the sample was cooled down at 78 K using a commercial liquid nitrogen cryostat. The sample was prepared in a thin-walled PMMA container. The spectrum was fitted by using the program WinNormos for the Igor6 software package.[29] Elemental analyses were carried out on an Elementar vario MICRO cube.

Lithium diisopropyl indenide 1a

Diisopropyl indene (6.0 g, 29.9 mmol) was dissolved in toluene and treated with *n*-butyl lithium (2.5 M in hexane, 12.0 mL,

29.9 mmol), whereby the colour of the solution turned orange. The mixture was stirred overnight at 353 K. **1a** precipitated as a solid and was collected by filtration and dried *in vacuo*. Recrystallisation from dimethoxyethane at 248 K yielded large crystals of **1a**·(dme).

Yield: 7.4 g, 25.0 mmol, 84%.

^{1}H NMR (400 MHz, C$_6$D$_6$, 295 K): δ (in ppm) = 1.55 (br s, 12 H, CH(CH$_3$)$_2$), 2.12 (s, 4 H, (CH$_2$OCH$_3$)$_2$), 2.42 (s, 6 H, (CH$_2$OCH$_3$)$_2$), 3.60 (sep, 2 H, CH(CH$_3$)$_2$), 6.58 (br s, 1 H, Ind–H), 7.05–7.09 (m, 2 H, Ind–H), 7.85–7.88 (m, 2 H, Ind–H).

^{13}C{^{1}H} NMR (101 MHz, C$_6$D$_6$, 295 K): δ (in ppm) = 25.8 (br d, CH(CH$_3$)$_2$), 27.5 (CH(CH$_3$)$_2$), 58.7 (dme), 69.4 (dme), 108.3 (Ind), 111.4 (Ind), 115.3 (Ind), 119.5 (Ind), 123.5 (Ind).

^{7}Li{^{1}H} NMR (156 MHz, C$_6$D$_6$, 295 K): δ (in ppm) = −8.8.

^{13}C{^{1}H} CP-MAS (13 kHz) NMR (101 MHz, 297 K): δ (in ppm) = 26.9 (CH(CH$_3$)$_2$), 58.4 (dme), 70.4 (dme), 108.2 (Ind), 111.9 (Ind), 115.1 (Ind), 115.7 (Ind), 117.9 (Ind), 122.9 (Ind).

^{7}Li{^{1}H} CP-MAS(10 kHz) NMR (156 MHz, 297 K): δ (in ppm) = −8.2.

Sodium di-*tert*-butyl indenide 1b

Di-*tert*-butyl indene (7.44 g, 32.6 mmol) was added to a suspension of sodium amide (1.33 g, 34.2 mmol) in thf. The mixture was heated to reflux for 7 h and subsequently stirred overnight at ambient conditions, turning from colourless to red brown. After filtration and evaporation of all volatiles, the residue was washed with small portions of hexane, and dried *in vacuo*.

Yield: 6.0 g, 23.8 mmol, 73%.

Recrystallisation from dimethoxyethane at 248 K yielded crystals of **1b**·(dme)$_3$.

^{1}H NMR (400 MHz, thf-D$_8$, 295 K): δ (in ppm) = 1.46 (s, 18 H, C(CH$_3$)$_3$), 6.32–6.36 (m, 2 H, Ind–H), 6.46 (s, 1 H, Ind–H), 7.52–7.56 (m, 2 H, Ind–H).

^{13}C{^{1}H} NMR (101 MHz, thf-D$_8$, 295 K): δ (in ppm) = 33.2 (C(CH$_3$)$_3$), 33.8 (C(CH$_3$)$_3$), 110.9 (Ind), 112.9 (Ind), 113.6 (Ind), 120.0 (Ind), 124.9 (Ind).

Germanocene 2a and stannocene 2b

A thf solution of sodium di-*tert*-butyl indenide **1b** (for **2a**: 0.25 g, 0.99 mmol; for **2b**: 1.00 g, 0.40 mmol) was treated with a thf solution of the corresponding group 14 salt (for **2a**: GeCl$_2$·dioxane: 0.12 g, 0.50 mmol; for **2b**: SnCl$_2$: 0.38 g, 2.0 mmol) at 193 K. The mixture was allowed to warm to room temperature and stirred overnight. All volatiles were removed *in vacuo*, the remaining solid residue was taken up in toluene and the resulting suspension was filtered. Subsequent removal of the solvent yielded the title compounds as yellow (**2a**) or orange (**2b**) solids. Crystals, suitable for single crystal X-ray diffraction, were obtained from toluene solutions at 248 K.

Yield **2a**: 153 mg, 0.29 mmol, 58%; **2b**: 0.40 g, 0.70 mmol, 35%.

2a: CHN for C$_{34}$H$_{46}$Ge: C 76.10 (calc.: 77.44); H 9.10 (calc.: 8.79)%.

^{1}H NMR (400 MHz, C$_6$D$_6$, 295 K): δ (in ppm) = 1.34 (s, 36 H, C(CH$_3$)$_3$), 5.92 (s, 2 H, Ind–H), 6.92–6.97 (m, 4 H, Ind–H),

7.48–7.52 (m, 4 H, Ind–H). ^{13}C{^{1}H} NMR (101 MHz, C_6D_6, 295 K): δ (in ppm) = 32.3 (C(CH$_3$)$_3$), 32.5 (C(CH$_3$)$_3$), 115.3 (Ind), 121.6 (Ind), 122.5 (Ind), 125.2 (Ind), 129.5 (Ind).

2b: CHN for $C_{34}H_{46}Sn$: C 71.4 (calc.: 71.2); H 8.3 (calc.: 8.1)%.

^{1}H NMR (400 MHz, C_6D_6, 295 K): δ (in ppm) = 1.38 (s, 18 H, C(CH$_3$)$_3$), 6.02 (s, $^1J_{H–Sn}$ = 22 Hz, 2 H, Ind–H), 6.89–6.93 (m, 4 H, Ind–H), 7.51–7.56 (m, 4 H, Ind–H).

^{13}C{^{1}H} NMR (101 MHz, C_6D_6, 296 K): δ (in ppm) = 32.3 (C(CH$_3$)$_3$), 33.2 (C(CH$_3$)$_3$), 114.8 ($^1J_{C–Sn}$ = 49 Hz, Ind), 120.7 (Ind), 122.4 ($^1J_{C–Sn}$ = 11 Hz, Ind), 124.5 (Ind), 127.9 (Ind).

^{119}Sn{^{1}H} NMR (149 MHz, C_6D_6, 295 K): δ (in ppm) = −2272.

^{13}C{^{1}H} CP-MAS (13 kHz) NMR (101 MHz): δ (in ppm) = 31, 32, 33, 34 (C(CH$_3$)$_2$), 115 (Ind), 120 (Ind), 122 (Ind), 123 (Ind), 127 (Ind).

^{119}Sn{^{1}H} CP-MAS (13 kHz) NMR (149 MHz): δ_{iso} (in ppm) = −2335 (δ_{11} = −2216 ± 5, δ_{22} = −2318 ± 5, δ_{33} = −2470 ± 5).

^{119}Sn Mössbauer: δ = 3.80(1) mm s^{-1}; ΔE_Q = 0.70(1) mm s^{-1}; Γ = 0.81(1) mm s^{-1}.

Plumbocene 2c

A dme solution of sodium di-*tert*-butyl indenide **1b** (0.5 g, 2.00 mmol) was treated with a dme solution of PbBr$_2$ (0.367 g, 1.00 mmol) at 273 K. The mixture was allowed to warm to room temperature and stirred for 15 min. All volatiles were removed *in vacuo*, the remaining solid residue was taken up in toluene and the resulting suspension was filtered. Subsequent removal of the solvent yielded the title compound as a dark red solid. Crystals, suitable for single crystal X-ray diffraction, were obtained from an *ortho*-difluorobenzene solution at 248 K.

Yield: 0.315 g, 0.476 mmol, 48%.

CHN for $C_{34}H_{46}Pb$: C 59.42 (calc.: 61.69); H 7.10 (calc.: 7.00)%.

^{1}H NMR (400 MHz, C_6D_6, 294 K): δ (in ppm) = 1.39 (s, 36 H, C(CH$_3$)$_3$), 6.02 (s, $^1J_{H–Pb}$ = 26 Hz, 2 H, Ind–H), 6.88–6.92 (m, 4 H, Ind–H), 7.49–7.53 (m, 4 H, Ind–H).

^{13}C{^{1}H} NMR (101 MHz, C_6D_6, 294 K): δ (in ppm) = 31.4 (C(CH$_3$)$_3$), 34.2 (C(CH$_3$)$_3$), 112.5 ($^1J_{C–Pb}$ = 105 Hz, Ind), 120.2 (Ind), 121.7 (Ind), 127.0 (Ind), 128.8 (Ind).

^{207}Pb{^{1}H} NMR (83 MHz, C_6D_6, 294 K): δ (in ppm) = −4503.

^{13}C{^{1}H} CP-MAS (13 kHz) NMR (101 MHz): δ (in ppm) = 30, 31, 32, 34, 35 (C(CH$_3$)$_2$), 113 (Ind), 120 (Ind), 121 (Ind), 122 (Ind), 127 (Ind), 129 (Ind), 130 (Ind).

^{207}Pb{^{1}H} CP-MAS (13 kHz) NMR (83 MHz): δ_{iso} (in ppm) = −4734 (δ_{11} = −3891 ± 10, δ_{22} = −5169 ± 10, δ_{33} = −5169 ± 10).

Conflicts of interest

There are no conflicts to declare.

Acknowledgements

Notes and references

1 P. L. Pauson and G. Wilkinson, *J. Am. Chem. Soc.*, 1954, **76**, 2024–2026.

2 (*a*) T. J. Kealy and P. L. Pauson, *Nature*, 1951, **168**, 1039–1040; (*b*) S. A. Miller, J. A. Tebboth and J. F. Tremaine, *J. Chem. Soc.*, 1952, 632–635; (*c*) G. B. Kaufmann, *J. Chem. Educ.*, 1983, **60**, 185–186; (*d*) P. L. Pauson, *J. Organomet. Chem.*, 2001, **637–639**, 3–6; (*e*) H. Werner, *Angew. Chem., Int. Ed.*, 2012, **51**, 6052–6058.

3 (*a*) V. Cadierno, J. Díez, M. P. Gamasa, J. Gimeno and E. Lastra, *Coord. Chem. Rev.*, 1999, **193–195**, 147–205; (*b*) D. Zagrarian, *Coord. Chem. Rev.*, 2002, **233–234**, 157–176; (*c*) Y. Qian, J. Huang, M. D. Bala, B. Lian, H. Zhang and H. Zhang, *Chem. Rev.*, 2003, **103**, 2633–2690; (*d*) R. Leino, P. Lehmus and A. Lehtonen, *Eur. J. Inorg. Chem.*, 2004, 3201–3222; (*e*) V. B. Kharitonov, D. V. Muratov and D. A. Loginov, *Coord. Chem. Rev.*, 2019, **399**, 213027; (*f*) V. B. Kharitonov, Y. V. Nelyubina, I. D. Kosenko and D. A. Loginov, *J. Organomet. Chem.*, 2019, **880**, 312–316.

4 (*a*) P. Jutzi and N. Burford, Main Group Metallocenes, in *Metallocenes*, 1998; (*b*) M. A. Beswick, J. S. Palmer and D. S. Wright, *Chem. Soc. Rev.*, 1998, **27**, 225–232; (*c*) P. Jutzi and N. Burford, *Chem. Rev.*, 1999, **99**, 969–990; (*d*) P. H. M. Budzelaar, J. J. Engelberts and J. H. van Lenthe, *Organometallics*, 2003, **22**, 1562–1576.

5 M. J. Calhorda, C. C. Romão and L. F. Veiros, *Chem. – Eur. J.*, 2002, **8**, 868–875.

6 (*a*) A. H. Cowley, M. A. Mardones, S. Avendaño, E. Román, J. M. Manriquez and C. J. Carrano, *Polyhedron*, 1993, **12**, 125–127; (*b*) J. S. Overby, T. P. Hanusa and P. D. Boyle, *Angew. Chem., Int. Ed.*, 1997, **36**, 2378–2379; (*c*) J. N. Jones and A. H. Cowley, *Chem. Commun.*, 2005, 1300–1302.

7 (*a*) A. C. Möller, R. Blom, R. H. Heyn, O. Swang, C.-H. Görbitz and T. Seraidaris, *Eur. J. Inorg. Chem.*, 2005, 1759–1769; (*b*) X. Xu, Y. Chen and J. Sun, *Chem. – Eur. J.*, 2009, **15**, 846–850; (*c*) A. Glöckner, H. Bauer, M. Maekawa, T. Bannenberg, C. G. Daniliuc, P. G. Jones, Y. Sun, H. Sitzmann, M. Tamm and M. D. Walter, *Dalton Trans.*, 2012, **41**, 6614–6624.

8 R. Michel, R. Herbst-Irmer and D. Stalke, *Organometallics*, 2011, **30**, 4379–4386.

9 H. Gritzo, F. Schaper and H.-H. Brintzinger, *Acta Crystallogr., Sect. E: Struct. Rep. Online*, 2004, **E60**, m1108–m1110.

10 Low temperature ^{1}H NMR spectroscopy of **2a** at 243 K did not show any signal splitting, suggesting that the Ind–Ge bond rotation has a low energy barrier.

11 M. Grenz, E. Hahn, W.-W. du Mont and J. Pickardt, *Angew. Chem., Int. Ed. Engl.*, 1984, **23**, 61–63.

12 J. L. Atwood, W. E. Hunter, A. H. Cowley, R. A. Jones and C. A. Stewart, *J. Chem. Soc., Chem. Commun.*, 1981, 925–927.

13 C. Müller, D. M. Andrada, I.-A. Bischoff, M. Zimmer, V. Huch, N. Steinbrück and A. Schäfer, *Organometallics*, 2019, **38**, 1052–1061.

14 J. S. Overby, T. P. Hanusa and V. G. Young, *Inorg. Chem.*, 1998, **37**, 163–165.

15 C. Janiak, H. Schumann, C. Stader, B. Wrackmeyer and J. J. Zuckerman, *Chem. Ber.*, 1988, **121**, 1745–1751.

16 B. E. Eichler, B. L. Phillips, P. P. Power and M. P. Augustine, *Inorg. Chem.*, 2000, **39**, 5450–5453.

17 P. Jutzi, R. Dickbreder and H. Nöth, *Chem. Ber.*, 1989, **122**, 865–870.

18 (*a*) P. G. Harrison and J. J. Zuckerman, *J. Am. Chem. Soc.*, 1969, **91**, 6885–6886; (*b*) P. G. Harrison and M. A. Healy, *J. Organomet. Chem.*, 1973, **51**, 153–166; (*c*) S. Danés, C. Müller, L. Wirtz, V. Huch, T. Block, R. Pöttgen, A. Schäfer and D. M. Andrada, *Organometallics*, 2020, **39**, 516–527.

19 G. K. Shenoy and F. E. Wagner, *Mössbauer Isomer Shifts*, North-Holland Publishing Company, Amsterdam, 1978.

20 N. N. Greenwood and T. C. Gibb, *Mössbauer Spectroscopy*, Chapman and Hall Ldt., London, 1971.

21 J. J. Zuckermann, *Adv. Organomet. Chem.*, 1971, **9**, 21–134.

22 D. Honnick and J. J. Zuckerman, *Inorg. Chem.*, 1976, **15**, 3034–3037.

23 See ESI† for further details and references.

24 G. R. Fulmer, A. J. M. Miller, N. H. Sherden, H. E. Gottlieb, A. Nudelman, B. M. Stoltz, J. E. Bercaw and K. I. Goldberg, *Organometallics*, 2010, **29**, 2176–2179.

25 G. M. Sheldrick, *Acta Crystallogr., Sect. A: Found. Crystallogr.*, 2008, **64**, 112–122.

26 G. M. Sheldrick, *Acta Crystallogr., Sect. A: Found. Adv.*, 2015, **71**, 3–8.

27 G. M. Sheldrick, *Acta Crystallogr., Sect. C: Struct. Chem.*, 2015, **71**, 3–8.

28 C. B. Hübschle, G. M. Sheldrick and B. Dittrich, *J. Appl. Crystallogr.*, 2011, **44**, 1281–1284.

29 R. A. Brand, *WinNormos for Igor6 (version for Igor 6.2 or above: 22/02/2017)*, Universität Duisburg, Duisburg (Germany), 2017.